Wide Bandgap Light Emitting Materials and Devices

Edited by
Gertrude F. Neumark, Igor L. Kuskovsky,
and Hongxing Jiang

Wide Bandgap Light Emitting Materials and Devices

Edited by
Gertrude F. Neumark,
Igor L. Kuskovsky, and
Hongxing Jiang

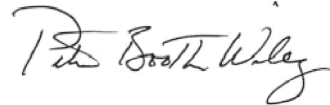## 1807–2007 Knowledge for Generations

Each generation has its unique needs and aspirations. When Charles Wiley first opened his small printing shop in lower Manhattan in 1807, it was a generation of boundless potential searching for an identity. And we were there, helping to define a new American literary tradition. Over half a century later, in the midst of the Second Industrial Revolution, it was a generation focused on building the future. Once again, we were there, supplying the critical scientific, technical, and engineering knowledge that helped frame the world. Throughout the 20th Century, and into the new millennium, nations began to reach out beyond their own borders and a new international community was born. Wiley was there, expanding its operations around the world to enable a global exchange of ideas, opinions, and know-how.

For 200 years, Wiley has been an integral part of each generation's journey, enabling the flow of information and understanding necessary to meet their needs and fulfill their aspirations. Today, bold new technologies are changing the way we live and learn. Wiley will be there, providing you the must-have knowledge you need to imagine new worlds, new possibilities, and new opportunities.

Generations come and go, but you can always count to Wiley to provide you the knowledge you need, when and where you need it!

William J. Pesce
President and Chief Executive Officer

Peter Booth Wiley
Chairman of the Board

Wide Bandgap Light Emitting Materials and Devices

Edited by
Gertrude F. Neumark, Igor L. Kuskovsky,
and Hongxing Jiang

The Editors

Prof. Dr. Gertrude F. Neumark
Dept. of Applied Physics
Columbia University
1137, 500 W. 120th Street
New York, NY 10027
USA

Dr. Igor Kuskovsky
Department of Physics
Queens College of CUNY
65-30 Kissena Blvd.
Flushing, NY 11367
USA

Prof. Dr. Hongxing Jiang
Kansas State University
Department of Physics
Cardwell Hall
Manhattan, KS 66506-2601
USA

Cover
Courtesy of Andrei Osinsky, see also article by
John Muth and Andrei Osinsky in this book.

Wiley Bicentennial Logo
Richard J. Pacifico

© 2007 WILEY-VCH Verlag GmbH & Co. KGaA,
Weinheim

Contents

Preface

The most recent era of progress in semiconductor light emitting devices and materials started around 1990, with two independent developments. The first, in 1991 was a report by Haase et al. (Appl. Phys. Lett. **59** (1991) 1272) of the first blue-green laser diode, made from ZnSe and related alloys. The second, in 1994, was a report by Nakamura et al. (Appl. Phys. Lett. **64** (1994) 1687) of high-luminosity blue LED, from GaN and related alloys. Both of these followed very shortly after the achievement of good p-type ZnSe by Park et al. (Appl. Phys. Lett. **57** (1990) 2127) and p-type GaN by Amano et al. (Jpn. J. Appl Phys. **28** (1989) L2112) and by Nakamura et al. (Jpn. J. Appl Phys. **31** (1992) L139; **31** (1992) 1258), where it had been very difficult, for both materials, to obtain p-type conductivity.

Since then, progress in the GaN area has been spectacular, with estimated sales in 2006 of $5 Billion. LEDs have been produced in blue, violet, and UV as well as in high-brightness, with particular emphasis on white (via phosphors). These have a long life-time. They have a myriad uses, including traffic lights, automobile lightning, back-lightning for mobile phones, flashlights, lighting of superstructure of bridges, outdoor displays, etc. Lasers are being used for improved optical storage density and resolution (e.g., for DVDs) as well as for the ability for chemical- and biohazard substance detection.

Nevertheless despite all the successes of GaN based materials (e.g., UV and violet laser diodes for 390–420 nm and efficient LEDs to 530 nm), there are remaining problems, which are difficult to solve. Fundamental aspects are relatively poor p-type doping and lack of good substrates. Consequently, these materials have not given adequate emission in the important pure green (560–565 nm) spectral region. It is in this region that the human eye has its maximum response, with obvious applications to displays. Other important applications are white emission without phosphors and plastic optical fiber networks. This is why II-VI ZnSe-based wide bandgap materials remain of high interest. Spectral response of these materials in the deep green critical spectral region is excellent, although they also have the problem of p-type doping. It worth noting that white LEDs without phosphors, based on ZnSe alloys, with lifetime of 10,000 hours have recently been reported (T. Nakamura, Electr. Eng. Japn. **154** (2006) 42). In addition, there is high present

interest in ZnO for light emitting applications because of its large exciton binding energy (60 meV), which results in very efficient emission near the band edge at room temperatures as well as its relatively lower index of refraction, which permits more efficient extraction of light from ZnO due to the large critical angle for total internal reflection. However, numerous challenges remain in utilizing ZnO in lightning applications with the principal challenge being obtaining efficient p-type doping.

The present book consists of two parts, Part 1 on GaN and related issues and Part 2 on wide bandgap II-VIs. Articles in Part 1 discuss overall progress in nitride light emitters (Chapter 1), GaN-based LEDs on novel substrates (Chapter 2), and miniature GaN lasers (Chapter 3). Part 2 is devoted to II-VI wide bandgap compounds, specifically, ZnSeTe alloys (Chapter 4) and ZnO (Chapter 5).

Chapter 1 summarizes recent progress in III-Nitrides light emitters with the emphasis on UV laser and LEDs, including those fabricated from nonpolar oriented materials. Chapter 2 covers key growth issues, design considerations, and the operation of III–nitride LEDs on sapphire and other substrates, including Si, SiC, bulk GaN and AlN. In Chapter 3 the recent progress in III-nitride micro-size structures and light emitters, which are important for future optical circuit elements, is summarized with emphasis on fabrication and optical properties. Some of the applications of micro-emitters for boosting output power of LEDs are also discussed. Chapter 4 devoted to the latest developments in optical properties of Zn–Se–Te grown by migration enhanced epitaxy with sub-monolayer quantities of Te with focuses on ZnTe/ZnSe type-II QDs, including the observation of the optical Aharonov–Bohm effect. Chapter 5 summarizes optical properties of ZnO and its alloys, including very recent results on novel ZnCdO alloys. Special attention is paid to rarely discussed issues such as the index of refraction, including the methods used to measure it.

The Editors, July 2007

Contributors

Dr. Xian-An Cao
One Research Circle
GE Global Research Center
KWC 1811
Niskayuna, NY 12309
USA

Dr. Yi Gu
Department of Materials Science
    and Engineering
Northwestern University
Evanston, IL 60208
USA

Prof. Dr. Hongxing Jiang
Department of Physics
Kansas State University
Cardwell Hall
Manhattan, KS 66506-2601
USA

Dr. Igor Kuskovsky
Department of Physics
Queens College of CUNY
65-30 Kissena Blvd.
Flushing, NY 11367
USA

Prof. Jingyu Lin
Department of Physics
Kansas State University
Cardwell Hall
Manhattan, KS 66506-2601
USA

Dr. John Muth
North Carolina State University
ECE Dept, MRC Bldg. RM 234 E
2410 Campus Shore Drive
Raleigh, NC 27695
USA

Prof. Dr. Gertrude F. Neumark
Department of Applied Physics and
    Applied Mathematics
Columbia University
500 W. 120th Street, Rm. 1137
New York, NY 10027
USA

Dr. Andrei Osinsky
SVT Association, Inc.
7620 Executive Drive
Eden Prairie, MN 55344
USA

Dr. Tao T. Wang
Department of Electronic and
    Electrical Engineering
University of Sheffield
Mappin Street
Sheffield, S1 3JD
UK

Part I

1

III–Nitride Light-Emitting Diodes on Novel Substrates

Xian-An Cao

1.1
Introduction

During the past decade, III–nitrides, which form continuous and direct bandgap semiconductor alloys, have undergone a phenomenal development effort, and have emerged as the leading materials for light-emitting diodes (LEDs) with peak emission spanning from green through blue to ultraviolet (UV) wavelengths [1, 2]. High-brightness (HB) green and blue LEDs along with AlInGaP red and yellow LEDs complete the primary color spectrum and enable fabrication of large-scale full-color displays. Near-UV and blue LEDs, when used in conjunction with multiband or yellow phosphors, can produce white light and are therefore very attractive for solid-state lighting applications [3]. There are also plentiful ongoing endeavors to push emission wavelengths into the deep-UV regime for numerous applications including bioaerosol sensing, air and water purification, and high-density data storage.

One of the most defining features of the nitride material system is the lack of high-quality bulk GaN or AlN substrates. To date, all commercially available III–nitride LEDs are grown heteroepitaxially on foreign substrates such as sapphire and SiC. Si has also received some attention as the substrate for low-power LEDs due to its clear advantages of low cost and high quality. Many efforts have been devoted to developing high-quality buffer layers to accommodate the mismatch in lattice constant and thermal expansion coefficient between the epilayers and substrates. The presence of a high density of threading dislocations and large residual strain in the heteroepitaxial structures, along with strong piezoelectricity and large compositional fluctuation of the nitride alloys, give rise to some unique electrical and optical characteristics of current III–nitride LEDs [4].

Bulk GaN and AlN would be a nearly perfect match to LED heterostructures, and meet most substrate requirements. Homoepitaxial growth significantly reduces defect density and strain, and offers better doping and impurity control. These incentives are the driving force behind recent progress toward producing bulk GaN and AlN crystals [5, 6]. Some free-standing GaN substrates are now

commercially available, and preliminary results of homoepitaxy are encouraging. However, before large-area low-cost GaN wafers become available, sapphire and other foreign substrates will remain the common substrates for nitride LEDs due to the well-established heteroepitaxy technology.

In this chapter, key growth issues, design considerations, and the operation of III–nitride green, blue and UV LEDs on sapphire are described. An overview is then given that describes the growth and performance of nitride LEDs on other novel substrates, including Si, SiC, and bulk GaN and AlN. The influence of the substrates on the microstructural properties, electrical characteristics, light emission, and light extraction of the LEDs is discussed.

1.2
LEDs on Sapphire Substrates

1.2.1
LED Heteroepitaxy

Most commercially available III–nitride LEDs are grown on the *c*-plane of sapphire substrates. Large-area and high-quality sapphire is widely available in large quantities, and is fairly inexpensive. To date, much more knowledge and experience have been accumulated in the technology of growing III–nitrides on sapphire than on other substrates. Another advantage of using sapphire is its transparency to UV and visible light, reducing the parasitic light loss in the substrate. However, there are a few disadvantages associated with sapphire substrates. First, a large mismatch in lattice constant (~15%) and thermal expansion coefficient between nitride materials and sapphire gives rise to a high density of threading dislocations and biaxial stress in epitaxial layers. Second, sapphire is electrically insulating, making it necessary to fabricate LEDs in a lateral configuration. In this case, current spreading is a key device design consideration (described in Section 1.2.2). Third, sapphire has a relatively poor thermal conductivity, limiting heat dissipation in top-emitting LEDs. This, however, is less of a problem in flipchip LEDs, where heat is removed through the p-type contact.

Metal–organic chemical vapor deposition (MOCVD) has evolved as the dominant technique for growing III–nitride LEDs, not only on sapphire but also on other substrates [7]. However, the design of MOCVD reactors for nitrides is much less mature than for conventional III–V semiconductors. Currently both commercial and home-built reactors are used, and the growth process conditions vary widely. MOCVD is a nonequilibrium chemical process, in which gaseous precursors are injected from a precise gas-mixing manifold into a cold-wall reactor, where they react on a heated substrate. LED epitaxy is usually conducted under a low pressure. The common precursors include trimethylaluminum (TMAl), trimethylgallium (TMGa), and trimethylindium (TMIn) as the metal sources, and ammonia as the N source. Silane and bis-cyclopentadienyl-magnesium (Cp_2Mg) are used for n- and p-type doping, respectively. Hydrogen or nitrogen is used as the carrier gas.

The ideal growth temperatures for different layers of the LED structure are different: GaN is grown at 1000–1100 °C, AlGaN requires a slightly higher temperature, and InGaN is grown at a much lower temperature ~700–800 °C.

The realization of HB III–nitride LEDs on sapphire is based upon two epitaxy technology breakthroughs. The first was the demonstration of p-type conductivity in GaN. As-grown Mg-doped GaN has a very high resistivity due to the formation of Mg–H complexes. It was found that Mg can be activated by dissociating H from Mg using low-energy electron-beam irradiation [8] or annealing at >750 °C [9]. The second breakthrough was growing high-quality nitrides on sapphire using a thin low-temperature buffer layer [10]. The crystalline quality of GaN films grown directly on sapphire is generally poor due to the large mismatch between GaN and sapphire. Early work by several groups showed that GaN layers grown atop a thin AlN or GaN buffer layer greatly improved surface morphologies and crystalline quality [10, 11]. A buffer layer with a thickness of <100 nm, usually grown at ~500 °C, is critical to defect reduction and subsequent two-dimensional (2D) growth of device structures. Prior to the growth of the buffer, the sapphire substrate is usually nitridated by exposure to ammonia gas in the reactor [12, 13]. The nitridation process promotes GaN and AlN nucleation on sapphire and further improves the quality of the overlayer.

The first blue LED, reported by Nichia, consisted of InGaN/AlGaN double heterostructures (DHs) [14]. The active region was an InGaN layer codoped with Si and Zn, and an impurity-related transition was responsible for the blue emission. Their second-generation blue LEDs had an undoped InGaN single-quantum-well (SQW) active region, which exhibited efficient direct bandgap emission [15]. Figure 1.1(a) shows a typical layer structure of state-of-the-art green and blue LEDs, which consists of an InGaN/GaN multiple-quantum-well (MQW) active region [16, 17], an n-GaN lower cladding layer, a p-AlGaN upper cladding layer, and a p$^+$-GaN top contact layer. The p-AlGaN cladding layer is necessary to prevent electrons from escaping from the active region. The top surface is usually doped heavily with Mg to reduce the p-contact resistance. Similarly, deep-UV LEDs would have an AlGaN MQW active region sandwiched between n- and p-type AlGaN cladding layers with
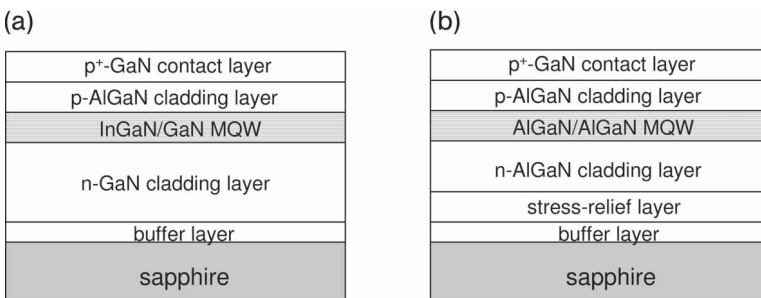

Fig. 1.1 Schematic of typical layer structures of state-of-the-art
(a) InGaN-based visible LEDs and (b) AlGaN-based UV LEDs
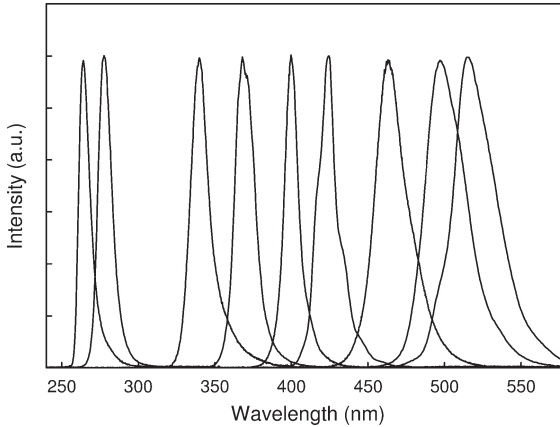on sapphire substrates.

Fig. 1.2 Electroluminescence spectra of III–nitride MQW LEDs grown on sapphire substrates using MOCVD.

a higher Al content (Fig. 1.1(b)) [18, 19]. Figure 1.2 illustrates a series of electroluminescence (EL) spectra of III–nitride MQW LEDs made on sapphire with the MOCVD technique and with peak emission ranging from green to deep-UV. The green and blue LEDs have a much larger full width at half-maximum (FWHM) of ~30 nm than the UV LEDs. The spectral broadening is believed to arise from large compositional inhomogeneity in the InGaN active regions [4].

During the LED overgrowth, the epilayer is essentially relaxed rather than being strained to lattice-match to the sapphire. However, a large biaxial compressive stress may be generated upon cooling to room temperature due to the larger thermal expansion coefficient of sapphire [20]. The actual magnitude and sign of the stress are a function of the growth conditions, and depend largely on the thickness and doping level of the thick n-type cladding layer. It has been found that excessive Si doping may change the stress from compressive to tensile [21], which promotes wafer bowing and film cracking, and limits the maximum size of wafers and the thickness of LED structures. Compared to GaN epilayers, AlGaN films grown on sapphire are more subject to a large residual stress. To improve strain management, state-of-the-art deep-UV LEDs are grown on a thick AlN template with an additional AlN/AlGaN superlattice stress-relief layer [18, 19]. Zhang et al. [22] reported a pulsed atomic-layer epitaxy technique, which considerably suppresses gas-phase reaction, enhances adatom surface migration, and produces AlN and AlGaN template layers with reduced alloy disorder and improved surface morphology. The high-quality stress-relief layer has proven to be crucial for the subsequent growth of High-Al content AlGaN LED structures.

Despite the use of a buffer layer to accommodate the large lattice mismatch between nitrides and sapphire, a very high level of threading dislocations (10^8–10^{10} cm^{-2}) is present within LED heterostructures [23]. Some traverse vertically from the epilayer/substrate interface to the top layer and, depending on the growth conditions of the capping layer, may terminate by forming various types of surface
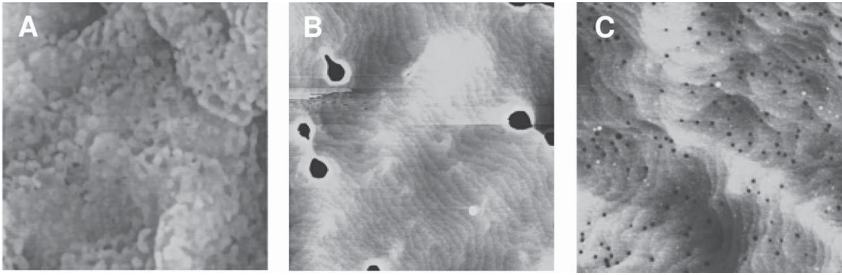
Fig. 1.3 AFM images (2 μm × 2 μm) of three representative InGaN/GaN MQW LEDs grown on sapphire using MOCVD.

defects. Figure 1.3 shows atomic force microscopy (AFM) images of three InGaN/GaN MQW LEDs on sapphire with different surface morphologies. The root-mean-square (rms) surface roughness of these samples is in the range of 0.4–0.8 nm over a $2 \times 2 \mu m^2$ area. The surface of LED A is microscopically rough but free of obvious pits, whereas LEDs B and C present a large number of surface defects. On sample B, there are $\sim 1.5 \times 10^8 \, cm^{-2}$ pits with hexahedral cone morphology and a size ~100 nm. LED C shows a swirled step structure and $4 \times 10^9 \, cm^{-2}$ small surface pits, which are caused by the intersection of the top surface with the dislocations [24]. Cross-sectional transmission electron microscopy (TEM) showed that the densities of dislocations reaching the MQW active region in LEDs A, B and C were $6 \times 10^8 \, cm^{-2}$, $3 \times 10^9 \, cm^{-2}$, and $5 \times 10^9 \, cm^{-2}$, respectively. In LED A, dislocation bending was found at 200–350 nm after the buffer layer, and a relatively small number of dislocations, mainly of edge character, propagated to the top layer. The hexagonal pits in LED B, usually called V-defects, were found to form in either the p-GaN capping layer or the MQW region, and were connected to threading dislocations. Large strain at the GaN/InGaN interfaces and In-rich regions [25, 26], or impurity complexes, are believed to be the cause of their formation [27].

The dislocation densities in III–nitride LEDs grown on sapphire are far higher than those observed in working LEDs based on conventional III–V semiconductors. GaAs-based LEDs with a dislocation density $>10^4 \, cm^2$ would not show any band-edge emission [28]. The fact that efficient blue and green LEDs can be made with highly defective InGaN materials suggests that threading dislocations do not act as efficient nonradiative recombination centers [29, 30]. This is supported by the finding that blue and green LEDs grown on a high-quality, laterally overgrown GaN template with a dislocation density of $\sim 7 \times 10^6 \, cm^{-2}$ had an external quantum efficiency similar to LEDs grown on a regular buffer layer [31]. It is now well accepted that In-rich quantum-dot-like (QD-like) regions self-formed in InGaN alloys due to strong compositional fluctuation, enhance carrier localization and radiative processes [4]. The localization effects, which are however lacking in high-quality AlGaN alloys, result in some unique EL behaviors of InGaN LEDs, and will be detailed in Sections 1.2.4 and 1.2.5.

1.2.2
Current Spreading

Due to the insulating substrate, InGaN/GaN LEDs grown on sapphire must be fabricated in a lateral configuration. A mesa is defined using plasma etching so that the n-type electrode can be deposited on the exposed n-GaN cladding layer, whereas the p-type contact is formed atop the p-GaN layer. The resistivity of the top p-GaN layer is typically several orders of magnitude higher than that of the n-type cladding layer. It is therefore necessary to add an additional conducting layer to spread current to regions not covered by the p-type bonding pad. In top-emitting LEDs, current spreading on the p-side usually relies on the use of a semitransparent contact covering the entire p-GaN [32, 33]. The current spreading layer also functions as an ohmic contact and light extraction window, and therefore must be transparent to the emitted light.

To reduce current nonuniformity, lateral current paths as determined by the spacing between the p-type and n-type electrodes should be smaller than the current spreading length, which is the length where current density drops to 1/e of that under the p-pad or at the mesa edge. The current spreading length L_s in a top-emitting LED is given by

$$L_s = \left(r_c + \rho_p t_p\right)^{1/2} \left|\frac{\rho_n}{t_n} - \frac{\rho_t}{t_t}\right|^{-1/2} \tag{1.1}$$

where ρ_p, ρ_n, ρ_t, t_p, t_n, and t_t are the respective resistivity and thickness of the p-GaN, n-GaN, and semitransparent contact, and r_c is the specific contact resistance of the p-contact [33]. It is clear that a uniform current distribution can be achieved when the n-type and p-type current spreaders have an identical sheet resistance (i.e., $\rho_t/t_t = \rho_n/t_n$) [32]. Current tends to crowd toward the p-pad or mesa edge adjoining the n-type electrode when this condition is not met. Current crowding may lead to a nonuniform light emission and self-heating, thus reducing the quantum efficiency and accelerating LED degradation. With increasing mesa size, current crowding becomes more severe. Novel mesa geometries, such as interdigitated mesas or multiple isolated mesas with a width less than L_s, must be used to alleviate this problem [34]. These types of designs also enjoy the advantage of good scalability, which is critical for developing large-area high-power LEDs.

A number of semitransparent contacts comprising a thin metal film have been investigated [35–39], among which a bilayer Ni/Au thin film is the most extensively used. It was found that the contact resistance of an Ni/Au contact to p-GaN can be substantially reduced by annealing the contact in an oxygen ambient to form NiO/Au [35]. The resultant NiO embedded with Au islands is believed to be a low-barrier contact to p-GaN [36], with a specific contact resistance in the 10^{-3}–$10^{-4}\,\Omega\,cm^2$ range. The oxidized Ni/Au is electrically conducive and semitransparent at visible wavelengths. Both the conductivity and transparency are strong functions of the Ni/Au content ratio. Figure 1.4 shows the sheet resistance and light transmission of Ni (5 nm)/Au films with varying Au thickness before and
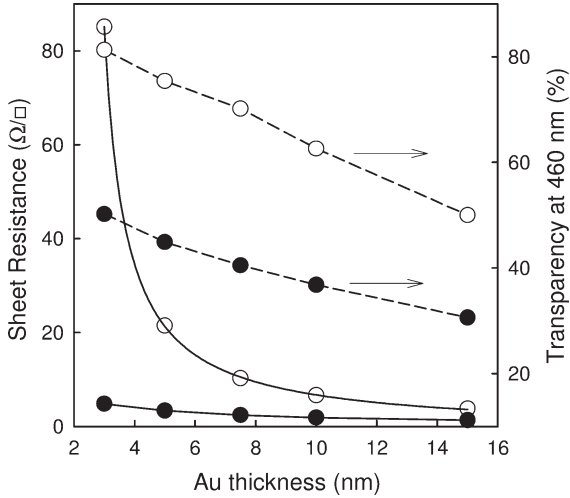
Fig. 1.4 Sheet resistance (solid lines) and light transmission (dashed lines) of Ni(5 nm)/Au films with varying Au thickness before (solid dots) and after (open dots) 550°C annealing in air.

after a 550°C anneal in air. The transparency is improved by ~60% after the anneal, and decreases rapidly with increasing Au thickness, whereas the resistance increases dramatically with decreasing Au content. Providing that the sheet resistance of the n-GaN layer in typical blue LEDs is ~20 Ω/□, the optimal Au thickness is 5–6 nm from the current spreading viewpoint. At this thickness, the Ni/Au film is >70% transparent at 460 nm, and forms a low-resistance ohmic contact to p-GaN.

In flipchip LEDs, the current on the p-side spreads in a thick ohmic metal, which also functions as a reflective mirror. Assuming negligible resistance of the p-metal, the current spreading length can be expressed as [40]:

$$L_s = \left((r_c + \rho_p t_p) \frac{t_n}{\rho_n} \right)^{1/2} \tag{1.2}$$

In this case, current tends to crowd at the edge of the mesa contact, and current density decreases exponentially with increasing distance from the mesa edge. Equation (1.2) shows that L_s can be increased by reducing the resistivity or increasing the thickness of the n-type cladding layer. In AlGaN-based deep-UV LEDs, L_s may be one order of magnitude smaller than in typical blue LEDs due to the low conductivity of high-Al AlGaN materials. Flipchip UV LEDs grown on sapphire are therefore more subject to current crowding and localized heating problems [41]. Interdigitated mesa structures or small mesa arrays must be employed to mitigate these problems.